THE IDEAL SHEAR STRENGTH OF FCC ALUMINUM UNDER SUPERIMPOSED TRIAXIAL STRESS FROM FIRST PRINCIPLES

M. Černý and J. Pokluda

Faculty of Mechanical Engineering., Brno University of Technology, Technická 2, CZ–616 69 Brno, Czech Republic

ABSTRACT

An influence of a triaxial stress applied perpendicularly to shear planes and shear direction during affine shear deformation of fcc crystals on the theoretical shear strength is studied for the $\langle 11\bar{2}\rangle\{111\}$ shear system using first principles methods. Al crystal is used as the case study. The applied relaxation procedure guarantees that the crystal is subjected to a superposition of shear, normal and in-plane stresses with individually adjustable in-plane and normal stress values. The theoretical shear strength of aluminum increases under the applied compressive normal stress or tensile in-plane stresses and vice versa. Crystal relaxations during shear reflect bonding features of Al.

KEYWORDS

Ideal shear strength, homogeneous deformation, ab initio calculations, fcc aluminum

INTRODUCTION

The theoretical shear strength (TSS) represents an important material characteristic since it determines the stress necessary for nucleation of dislocations. For this reason, TSS has been extensively studied in the last decade [1–6]. Most of the studies considered only a pure affine shear (with only one non-zero component of the stress tensor). Recent work of Jahnatek et al. [7] considered also so called alias pure shear and revealed an instability in Al crystal prior reaching the maximum shear stress in the affine pure regime that led to slight reduction of its TSS.

In practical applications, one can expect rather multiaxial stress state. Therefore, certain attention has been paid also to shear of fcc [3, 8–11] and bcc [12, 13] metals and covalent crystals [14] under superimposed normal stresses. At the atomistic scale, similar loading conditions can be expected in nanoindentation experiments in certain critical volumes of crystals under the indentor tip [15]. Therefore, a process of dislocation nucleation in the vicinity of nanoindentors can be studied in terms of the theoretical shear strength under superimposed normal stresses [16]. The shear strength seems also to control the limit of crystal stability under uniaxial loading since the crystal latices prefer a failure by shear in convenient shear system to that by a tensile instability [17, 18].

Former results on the influence of normal stresses on TSS predicted that the shear strength mostly raises under superimposed compressive normal stress and decreases under tensile normal stresses [3, 9–13]. The obtained dependences were mostly monotonous functions of the normal stress. Certain exception represented fcc Cu, where TSS was lowered by tensile normal stresses, whereas, in contrast to other elements, it was lowered also by compressive

normal stresses [10]. The phenomenon was explained by crystal relaxation during the shearing process. Copper crystal prefers to extend the shear planes (perpendicularly to the shear direction) rather than increase their interplanar separation [1, 3, 10, 11]. An application of an additional compressive normal stress contributes to further lateral extension that makes the shear deformation easier [3, 10, 11]. The first systematic study of TSS in fcc crystals under independently adjustable normal stresses that act normally (normal stress) and parallel (in-plane stresses) to shear planes [11] for Ni, Cu, Ir, and Pt revealed qualitative differences between responses of individual elements reflecting their electronic structures. In the special case of hydrostatic loading, however, these functions were found to be qualitatively uniform.

In the present study, ab initio simulations of a uniform shear deformation are performed for fcc aluminum crystal subjected to a superposition of shear and normal stresses. The main aim is to evaluate an influence of the normal stresses to TSS in Al and to compare the results to those for the previously investigated elements [11]. The attention is paid to the $\langle 11\bar{2}\rangle\{111\}$ shear system that represents the most favorable shear in fcc crystals.

COMPUTATIONAL DETAILS

The Al crystal was subjected to affine shear deformation in the $\langle 11\bar{2}\rangle\{111\}$ shear system. Normal stresses (compressive or tensile) were superimposed to the shear stress and kept constant along the whole shear deformation path. In consistence to Ref. [11], the axes x, y, and z of our coordinate frame were conveniently oriented parallel to $[11\bar{2}]$, $[\bar{1}10]$ and $[111]$ crystallographic directions.

Also the computational procedure based on ab initio calculations of a stress tensor (using Hellman-Feynman theorem) started from the equilibrium (unstressed) state. Then, the simulation cell was optimally strained in order to converge the stress tensor (with allowed tolerance of ± 0.2 GPa) to a state with $\sigma_1 = \sigma_2 = \sigma_p$ (normal in-plane stresses that force the planes to shrink or to extend), $\sigma_3 = \sigma_n$ (the normal stress that pushes together (or pulls apart) the shear planes), $\sigma_5 = \tau$ (the resolved shear stress) and $\sigma_4 = \sigma_6 = 0$. Calculations were repeated in several cycles for set of preset values of σ_n and σ_p.

At the beginning of any computational cycle, the τ value was zero. Consequently, the (111) planes were incrementally sheared in the $[11\bar{2}]$ direction and the stresses were relaxed in the described way with the exception of the shear stress τ. This stress was not directly controlled by our computational procedure and its values reflected the applied (engineering) shear strain γ. Each computational cycle yielded τ as a function of γ with a maximum stress value τ_{max} that refers to the theoretical shear strength under the superimposed normal stresses σ_n and σ_p.

The necessary stresses for our relaxation procedure were computed by using the Vienna Ab initio Simulation Package (VASP) [19, 20]. This first-principles computational code utilizes a plane wave basis set and pseudo-potential approach with ultra-soft pseudo-potentials of Vanderbilt type [21]. The exchange-correlation energy contribution was evaluated using the generalized-gradient approximation of Perdew and Wang [22]. The $31\times31\times31$ k-points mesh was found to be necessary to get a good convergence and good agreement with the experimental elastic moduli. The cutoff energy for the plane wave basis set was set to 170 eV. The solution was considered to be self-consistent when the energy difference of two consequent iterations was smaller than 10 μeV.

RESULTS AND DISCUSSION

Table 1 contains calculated values of the ground-state properties for aluminum (the equilibrium lattice parameter a_0, the bulk modulus B and the $\langle 11\bar{2}\rangle\{111\}$ shear modulus G) that are compared with available experimental and literature data. The added calculated values of the maximum shear stress τ^0_{max} and the corresponding values of the engineering shear strain γ^0_{max} for $\sigma_p = \sigma_n = 0$ correspond to TSS values and the critical strains from pure affine shear process. The shear modulus G was calculated from the $\tau(\gamma)$ dependence under the conditions $\sigma_n = \sigma_p = 0$ in our optimization procedure. The experimental B and G values corresponding to fully relaxed shear in the considered system were determined from elastic constants [23].

Table 1: Computed values of the equilibrium lattice parameter a_0, the bulk modulus B, the shear modulus G, the theoretical shear strength τ^0_{max} and the corresponding critical engineering shear strain γ^0_{max} along with literature values.

	a_0	B	G	τ^0_{max}	γ^0_{max}
calc.	4.05	74	30	2.9	0.19
expt. [23]	4.05	76	25		
Ref. [5]	4.04		27	2.8	0.20
Ref. [7]			28	2.8	0.19

As can be seen from Table 1, the computed equilibrium lattice parameters matches the experimental value. The computed bulk modulus agrees with the experimental one within 3%, however, the shear modulus is overestimated by 20%. On the other hand, the G values collected from literature are in a better agreement with our calculated value. The TSS value and the critical shear strain also agree very well with the literature data.

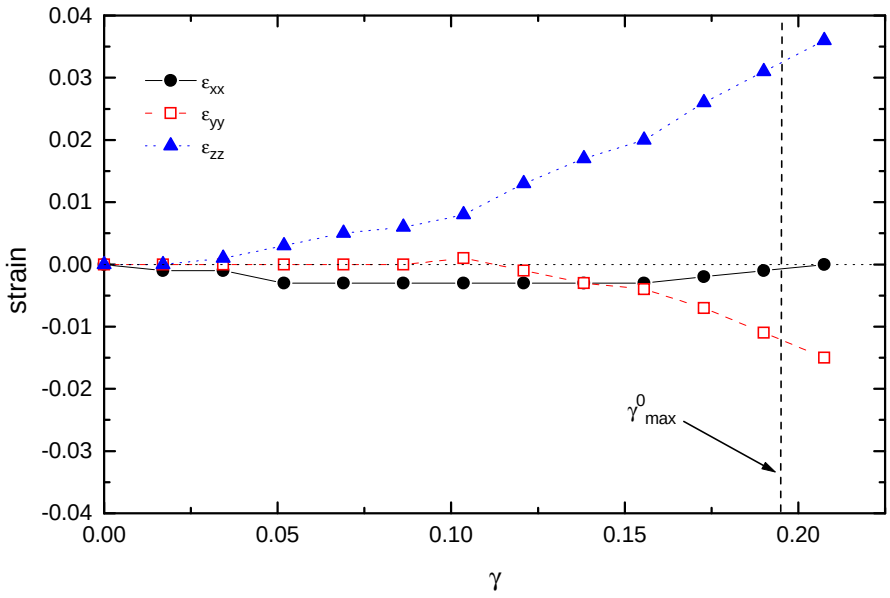

Figure 1: Evolution of normal strains ε_{xx} (circles), ε_{yy} (squares) and ε_{zz} (triangles) during shear deformation in Al crystal.

The crystal relaxations during the pure shear are described in terms of the strains ε_{xx} (a contraction of the shear planes along the shear direction), ε_{yy} (perpendicular extension or contraction of the planes in $[\bar{1}10]$ direction) and ε_{zz} (an increase of the inter-planar distance) in Fig. 1. The strains are plotted as functions of the shear strain γ (under $\sigma_n = \sigma_p = 0$) up to its critical

value γ^0_{max}. It can be seen that the aluminum crystal prefers an increase of the shear planes distance to any other relaxations in agreement with observation of Ogata et al. [3]. An extension in $[\bar{1}10]$ direction is almost negligible at small strains while for strains higher than 10% the crystals contracts which reminds relaxations of Pt crystal [11]. On the other hand, its contractions in $[11\bar{2}]$ direction are relatively small and vanishing at γ^0_{max}. The ratio E_{111}/E_{110} for Al is approximately 1.1 (similarly to the ratios for Ir and Pt [11]) which is reflected by the relatively large increase of the inter-planar distance whereas the strains ε_{xx} and ε_{yy} are smaller.

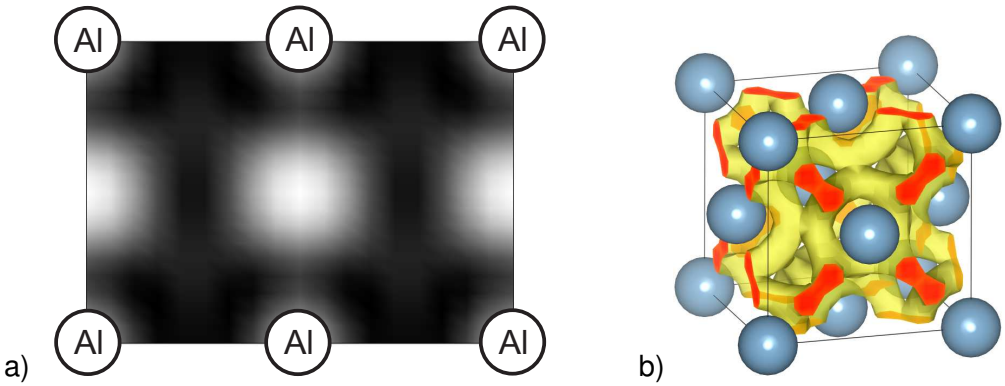

Figure 2: a) 2D map of the valence electron localization function in $(\bar{1}10)$ planes of the Al crystal. The darker regions are those with higher ELF values. b) ELF surface for the iso-value of 0.6.

The electrons in Al are localized in the form of a pipe-like channels [24, 25]. This can be illustrated in Fig. 2 that presents a 2D plot of an electron localization function (ELF) for valence electrons within $(\bar{1}10)$ planes and an ELF iso-surface (for the value of 0.6) of unstressed aluminum crystal. Topological analysis of ELF can be used for characterization of bonding properties of materials [26, 27]. Similarly as in our previous work [11], the ELF was calculated directly by the VASP code and the obtained output files were visualized using a VESTA package [28]. It should be noted that the maximum ELF value (above 0.6) is significantly higher that the maxima in Ni, Cu, Ir and Pt (below 0.4) [11] that demonstrates relatively strongly covalent character of bonding in Al reported already by Ogata et al. [5] or Kamran et al. [25] and attributed to $s-p$ hybridization of its electrons.

The computed values of the maximum shear stress τ_{max} (i.e. TSS) are plotted in Fig. 3 as functions of the normal stress σ_n for three constant values of in-plane stresses σ_p. To make the results consistent with those published previously for Ni, Cu, Ir and Pt, the open symbols and the dashed lines connect data-points corresponding to tensile in-plane stresses σ_p, whereas the solid symbols and the solid lines display data from the compressive region of σ_p. As can be seen from Fig. 3, the influence of in-plane stresses σ_p on TSS is lower than that of the normal stress σ_n, and the results are similar to those reported for Ir or Pt, where TSS is raised (lowered) by the compressive (tensile) σ_n and lowered (raised) by the compressive (tensile) σ_p.

CONCLUSIONS

Atomistic modeling of a pure affine shear in the $\langle 111\rangle\{11\bar{2}\}$ system in fcc aluminum under superimposed triaxial normal stresses was performed using ab initio calculations. The theoretical shear strength was computed for several combinations of individually adjustable values of normal and in-plane stresses. The results show that the theoretical shear strength increases (almost linearly) with increasing compressive normal stress and decreases under tensile normal stress. The opposite trends can be seen for influence of in-plane stresses. This behavior

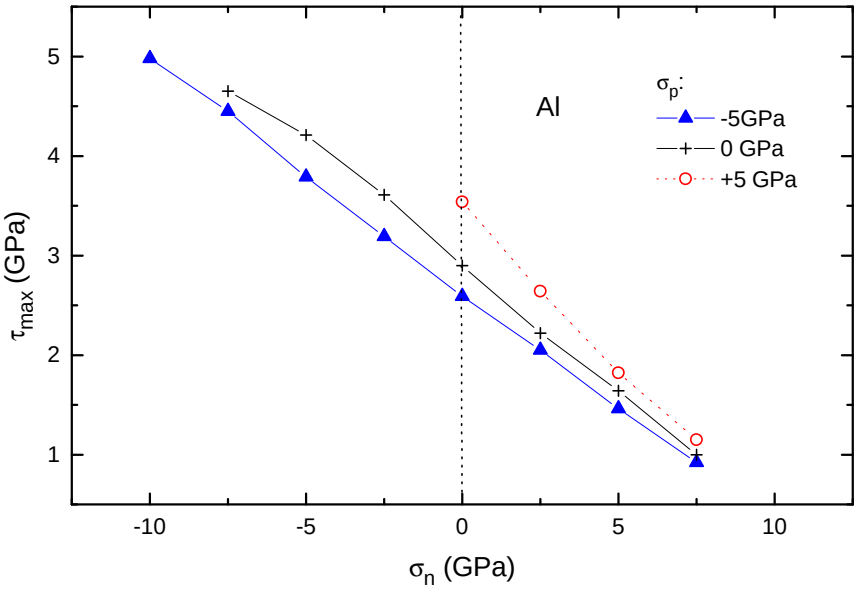

Figure 3: Theoretical shear strength τ_{max} as a function of the superimposed normal stress σ_n at three different values of the in-plane stress σ_p (see the figure legend).

can be qualitatively understood in terms of the electronic structure.

ACKNOWLEDGEMENT

Authors acknowledge the financial support of the Ministry of Education, Youth and Sports of the Czech Republic (project MSM 0021630518).

REFERENCES

[1] C. R. Krenn, D. Roundy, J. W. Morris Jr., M. L. Cohen, The non-linear elastic behavior and ideal shear strength of Al and Cu, Mater. Sci. Eng. A 317 (1) (2001) 44-8.
[2] Y. Umeno, T. Kitamura, Ab initio simulation on ideal shear strength of silicon, Mater. Sci. Eng. B 88 (2002) 79-84.
[3] S. Ogata, J. Li, S. Yip, Ideal pure shear strength of aluminum and copper, Science 298 (2002) 807.
[4] D. M. Clatterbuck, D. C. Chrzan, J. W. Morris, Jr., The ideal strength of iron in tension and shear, Acta Mater. 51 (2003) 2271.
[5] S. Ogata, J. Li, N. Hirosaki, Y. Shibutani, S. Yip, Ideal shear strain of metals and ceramics, Phys. Rev. B 70 (2004) 104104.
[6] Y.-L. Liu, Y. Zhang, H.-B. Zhou, G.-H. Lu, M. Kohyama, Theoretical strength and charge redistribution of fcc Ni in tension and shear, J. Phys.: Condens. Matter 20 (2008) 335216.
[7] M. Jahnátek, J. Hafner, M. Krajčí, Shear deformation, ideal strength, and stacking fault formation of fcc metals: A density-functional study of Al and Cu, Phys. Rev. B 79 (22) (2009) 224103.
[8] A. Kelly, W. R. Tyson, A. H. Cottrell, Ductile and brittle crystals, Phil. Mag. 15 (1967) 567-581.
[9] M. Černý, J. Pokluda, Influence of normal stress on theoretical shear strength of fcc metals, Mater. Sci. Eng. A 483-484 (2008) 692-694.

[10] M. Černý, J. Pokluda, Influence of superimposed normal stress on the $\langle 112\rangle\{111\}$ shear strength in perfect fcc metals, Comp. Mater. Sci. 44 (2008) 127-130.
[11] M. Černý, J. Pokluda, The theoretical shear strength of fcc crystals under superimposed triaxial stress, Acta Mater. (in print).
[12] P. Söderlind, J. A. Moriarty, First-principles theory of Ta up to 10 Mbar pressure: Structural and mechanical properties, Phys. Rev. B 57 (1998) 10340.
[13] M. Černý, P. Šesták, J. Pokluda, Influence of superimposed normal stress on shear strength of perfect bcc crystals, Comput. Mater. Sci. 47 (2010) 907910.
[14] Y. Umeno, M. Černý, Effect of normal stress on the ideal shear strength in covalent crystals, Phys. Rev. B 77 (2008) 100101.
[15] T. Zhu, J. Li, K. J. Vliet, S. Ogata, S. Yip, S. Suresh, Predictive modeling of nanoindentation-induced homogeneous dislocation nucleation in copper, J. Mech. Phys. Solids 52 (2004) 691-724.
[16] J. Horníková, P. Šandera, M. Černý, J. Pokluda, Multiscale modelling of nanoindentation test in copper crystal, Eng. Fract. Mech. 76 (2008) 37553762.
[17] F. Milstein, S. Chantasiriwan, Theoretical study of the response of 12 cubic metals to uniaxial loading, Phys. Rev. B 58 (1998) 6006-6018.
[18] M. Černý, J. Pokluda, The theoretical tensile strength of fcc crystals predicted from shear strength calculations, J. Phys.: Condens. Matter 21 (2009) 145406.
[19] G. Kresse, J. Hafner, Norm-conserving and ultrasoft pseudopotentials for first-row and transition elements, J. Phys.: Condens. Matter 6 (40) (1994) 8245-8257.
[20] G. Kresse, J. Furthmüller, Efficient iterative schemes for ab initio total-energy calculations using a plane-wave basis set, Phys. Rev. B 54 (16) (1996) 11169-11186.
[21] D. Vanderbilt, Soft self-consistent pseudopotentials in a generalized eigenvalue formalism, Phys. Rev. B 41 (11) (1990) 7892-7895.
[22] J. P. Perdew, Y. Wang, Accurate and simple analytic representation of the electron-gas correlation energy, Phys. Rev. B 45 (23) (1992) 13244-13249.
[23] D. R. Lide (Ed.), Handbook of Chemistry and Physics, 86th Edition, CRC Press, 2005.
[24] S. Kamran, K. Chen, L. Chen, L. Zhao, Electronic origin of anomalously high shear modulus and intrinsic brittleness of fcc Ir, Journal of Physics: Condensed Matter 20 (8) (2008) 085221.
[25] S. Kamran, K. Chen, L. Chen, Ab initio examination of ductility features of fcc metals, Phys. Rev. B 79 (2) (2009) 024106.
[26] B. Silvi, A. Savin, Classification of chemical bonds based on topological analysis of electron localization functions, Nature 371 (1994) 683-686.
[27] B. Silvi, C. Gatti, Direct space representation of the metallic bond, J. Phys. Chem. A 104 (5) (2000) 947-953.
[28] K. Momma, F. Izumi, *VESTA*: a three-dimensional visualization system for electronic and structural analysis, Journal of Applied Crystallography 41 (3) (2008) 653-658.

Corresponding author: cerny.m@fme.vutbr.cz